Effect of grain size on grain boundary strengthening of copper bicrystals under cyclic loading

Z. F. Zhang, Z. G. Wang, and Y. M. Hu

To clarify the strengthening effect of grain boundaries (GB), cyclic deformation behaviour of really grown [$\bar{4}79$]‖[$\bar{1}25$] copper bicrystals with different widths (4, 6, and 8 mm, denoted RB-4, RB-6, and RB-8) of component crystals and a combined copper bicrystal (denoted CB-6), obtained by sticking component single crystals G1 [$\bar{4}79$] and G2 [$\bar{1}25$] together, was investigated. The results showed that the cyclic saturation stresses increased in the order of bicrystals of CB-6 < RB-8 < RB-6 < RB-4. It is indicated that the GB effect caused different degrees of strengthening, which increased with the decreasing width of the RB bicrystals. By surface observation, it was found that only the primary slip system was activated in the combined bicrystal during cyclic deformation. However, an additional slip system appeared near the GB within the crystal G2 [$\bar{1}25$] in the RB bicrystals (except in the primary slip system), and formed a GB affected zone (GBAZ). The width of the GBAZ was about 400 and 600 μm at plastic strain amplitudes of 0·1% and 0·2% respectively. Meanwhile, using an electron channelling contrast (ECC) technique in the SEM, the dislocation patterns near the GB and within the component crystals were observed. It was found that a two phase structure of persistent slip bands (PSBs) and matrix (or veins) can form in these bicrystals, similar to that in copper single crystals. But these PSBs cannot transfer through the GB during cyclic deformation. Based on the results above, the effect of grain size on GB strengthening of copper bicrystals was discussed.

MST/4267

The authors are in the State Key Laboratory for Fatigue and Fracture of Materials, Institute of Metal Research, Chinese Academy of Sciences, Shenyang, 110015, China. *Manuscript received 2 November 1998; accepted 13 August 1999.*

Introduction

It is well-known that a copper single crystal, oriented for single slip, exhibits a plateau region over a wide range of resolved shear plastic strain from $6{\cdot}0 \times 10^{-5}$ to $7{\cdot}5 \times 10^{-3}$ in its cyclic stress–strain (CSS) curve.[1,2] Cheng and Laird[3] found that the plateau saturation resolved shear stress at room temperature was in the range of 28–30 MPa, which represented the critical stress activating persistent slip bands (PSBs). Meanwhile, cyclic deformation behaviour of copper polycrystals has been widely investigated. Some investigators found that the CSS curves of some copper polycrystals also displayed the plateau feature over a certain strain range.[4–7] However, Mughrabi[8] and Lukas and Kunz[9] urged that there should be no apparent plateau in the CSS curve of copper polycrystals. To clarify the controversy about the CSS curves between copper single and polycrystals, it seems that the following questions should be answered:

(i) can PSBs also form in the interior of polycrystals under cyclic loading?
(ii) is the stress–strain response of the polycrystal a simple average over all the grains during cyclic deformation?
(iii) does the strain compatibility requirement lead to a grain boundary affected zone (GBAZ) with secondary or multiple slip near the grain boundary (GB) during cyclic deformation?
(iv) is the stress affected by the GBAZ and grain size in polycrystals?

Since PSBs were observed in the interior of polycrystalline copper[10] and stainless steel[11] by TEM, the two-phase model proposed by Winter *et al.*[12] was also accepted in polycrystals. By comparing the cyclic deformation behaviour of mono- and polycrystals,[13] however, it was suggested that the stress–strain response is not a simple average over all the grains. The reason for this is that the grains in polycrystals do not deform independently. Rey and Zaoui[14,15] and Mirura *et al.*[16,17] found that a GBAZ existed, which had a strengthening effect on copper and aluminium bicrystals. In addition, Margolin *et al.*[18–20] also proposed a GB strengthening mechanism in β brass bicrystals. Unfortunately, there are few studies dealing with the GB strengthening effect under cyclic deformation. Recently, cyclic deformation behaviour of [$\bar{1}35$]‖[$\bar{1}35$], [$\bar{1}35$]‖[$\bar{2}35$], [$\bar{2}35$]‖[$\bar{2}35$], and [$\bar{6}79$]‖[$\bar{1}45$] copper bicrystals[21,22] with a parallel GB were investigated and an apparent GB strengthening effect was observed. However, the size of these copper bicrystals is constant and the grain size effect was not involved. In the present study, two kinds of copper bicrystal specimens were designed, i.e. really grown bicrystal specimens (RB) with different widths and a combined copper bicrystal (CB) with the component crystals G1 and G2 in parallel. The aim of the present study is to further investigate the grain size effect of GB strengthening on copper bicrystals.

Experimental procedure

A bicrystal plate of size 120 × 25 × 15 mm was grown from oxygen free, high conductivity copper (OFHC) of 99·999% purity by the Bridgman method in a horizontal furnace, and the GB was along the growing direction. In order to distinguish the grain size effect of GB strengthening in the copper bicrystals during cyclic deformation, two kinds of bicrystal specimens were made by spark cutting from the grown bicrystal plate. They are (a) fatigue specimens of really grown copper bicrystals with a parallel GB and different component crystal widths of 2 + 2 mm (RB-4), 3 + 3 mm (RB-6), and 4 + 4 mm (RB-8), as shown in Fig. 1*a*; (b) fatigue specimens of combined bicrystals obtained by sticking the component crystals G1 and G2 together at the grip parts, as indicated in Fig. 1*b*. By electron backscattering diffraction (EBSD) in the SEM, the crystallographic relationships of two component crystals were

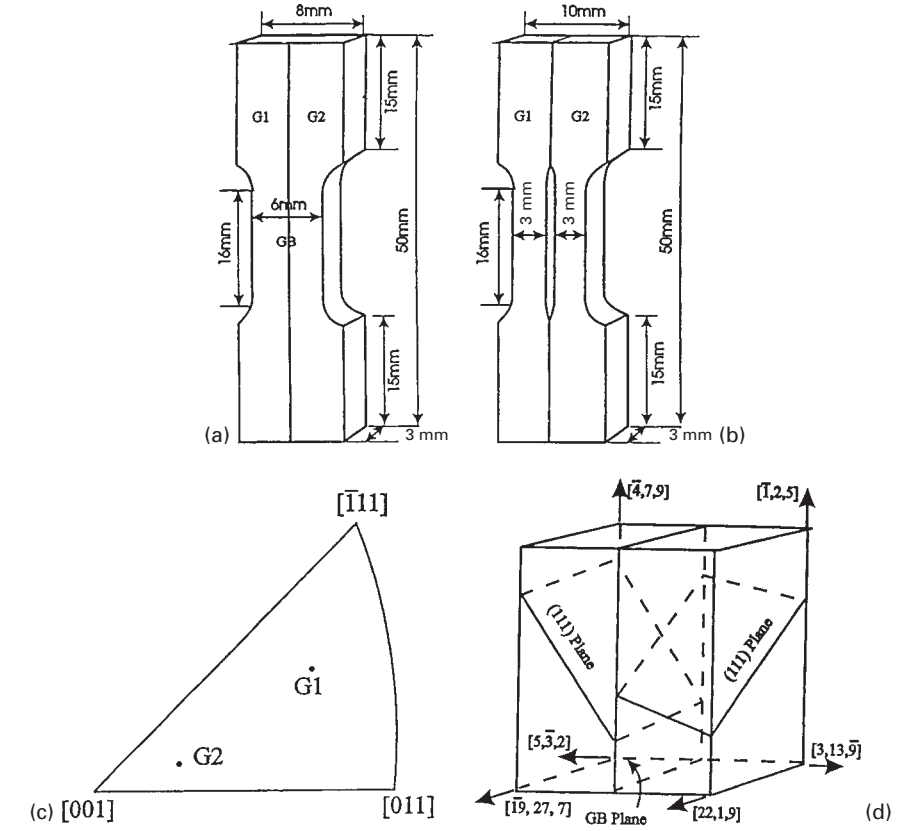

a really grown bicrystal (RB); *b* combined bicrystal (CB); *c* crystallographic orientations of crystals G1 and G2; d crystallographic relationships of bicrystals RB and CB

1 Fatigue specimens and orientations of copper bicrystals

determined, and are listed as follows

$$G1 = \begin{pmatrix} 0{\cdot}1878 & -0{\cdot}3310 & 0{\cdot}9235 \\ 0{\cdot}8140 & 0{\cdot}5793 & 0{\cdot}0422 \\ -0{\cdot}5496 & 0{\cdot}7448 & 0{\cdot}3775 \end{pmatrix}$$

$$= \begin{pmatrix} 3 & -4 & 22 \\ 13 & 7 & 1 \\ -9 & 9 & 9 \end{pmatrix}$$

$$G2 = \begin{pmatrix} 0{\cdot}8058 & -0{\cdot}1826 & -0{\cdot}5628 \\ -0{\cdot}4766 & 0{\cdot}3651 & -0{\cdot}8002 \\ 0{\cdot}3515 & 0{\cdot}9129 & 0{\cdot}2075 \end{pmatrix}$$

$$= \begin{pmatrix} 5 & -1 & -19 \\ -3 & 2 & -27 \\ 2 & 5 & 7 \end{pmatrix}$$

Figure 1*c* shows the stress axis orientations of the two component crystals. Clearly, both of them are oriented for single slip and have different Schmid factors of $\Omega_{G1} = 0{\cdot}436$ and $\Omega_{G2} = 0{\cdot}490$, respectively. The more detailed crystallographic relationships of the bicrystal are shown in Fig. 1*d*. Before cyclic deformation, all the specimens were electropolished carefully for surface observation. Cyclic push–pull tests were performed on a Shimadzu servohydraulic testing machine under plastic strain control at room temperature and in air. A triangle wave with a frequency of 0·2 Hz was used. The applied axial plastic strain amplitudes ε_{pl} were 0·1% and 0·2%. Peak loads in tension and compression and hysteresis loops were recorded by computer automatically. After cyclic saturation, the slip morphology was observed by SEM, especially in the vicinity of the GB.

Recently, the electron channelling contrast (ECC) technique in the SEM has been successfully applied to study the dislocation patterns in deformed metals,[23–29] such as stainless steel,[29] nickel,[23–25] and copper.[26,30,31] It has been generally recognised that the SEM–ECC technique can reveal some information which is difficult to achieve by conventional TEM techniques. For example, it allows the observation of dislocation patterns over the whole cross-section of the specimen, and especially at some specific sites, such as in the vicinity of GB[30,31] and deformation bands.[23] Therefore, the fatigued dislocation patterns of these copper bicrystals were also observed by this technique. The surface slip traces of the bicrystals were removed by careful electropolishing to observe the dislocation patterns within grains and near the GB using the SEM-ECC technique.

Experimental results

CYCLIC HARDENING AND SATURATION BEHAVIOUR

Figure 2*a* and *b* shows the cyclic hardening curves of the [$\bar{4}$79]‖[$\bar{1}$25] bicrystals RB-8, RB-6, RB-4, and CB-6 at the axial plastic strain amplitudes ε_{pl} of 0·1% and 0·2%, respectively. The axial saturation stresses σ_{as} are listed in Table 1. It can be seen that all the bicrystals exhibited rapid initial hardening and saturation with different saturation stresses. First, the saturation stress of the bicrystal CB was always lowest among these bicrystals, indicating that the GB should play a strengthening role in the bicrystals RB. This result is consistent with that in [$\bar{1}$35]‖[$\bar{1}$35], [$\bar{1}$35]‖[$\bar{2}$35], [$\bar{2}$35]‖[$\bar{2}$35], and [$\bar{6}$79]‖[$\bar{1}$45] copper bicrystals.[21,22] Second, the axial saturation stresses increased in the order of CB-6 < RB-8 < RB-6 < RB-4 at the same strain amplitude. This implies that the GB strengthening effect on the bicrystals

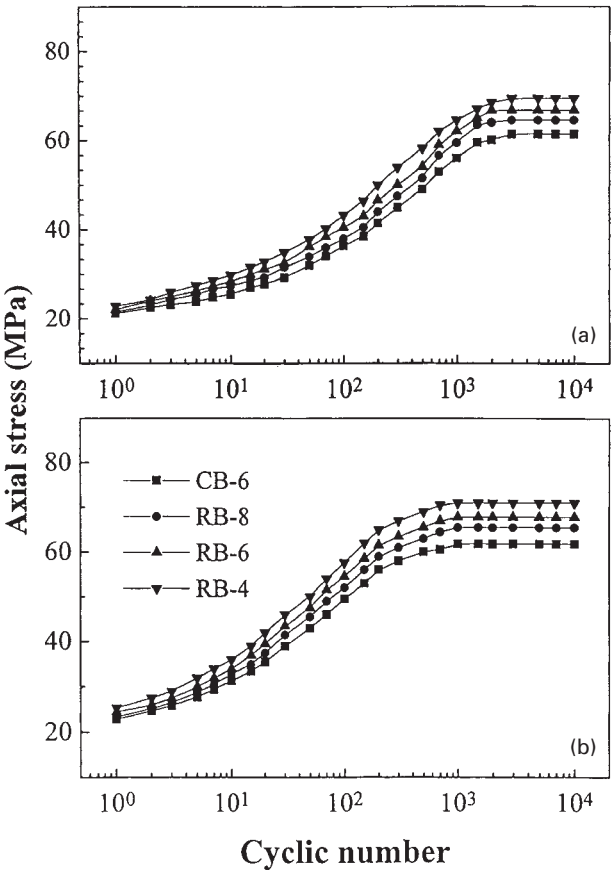

a $\varepsilon_{pl} = 0{\cdot}1\%$; *b* $\varepsilon_{pl} = 0{\cdot}2\%$

2 Cyclic hardening curves of bicrystals CB and RB at different strain amplitudes

RB should be associated with the grain size of the component crystals and will be discussed below in the section on 'Surface slip morphology'.

SURFACE SLIP MORPHOLOGY

By SEM, the following features of slip morphology in the bicrystals can be observed:

(i) only the primary slip system was activated in the bicrystal CB-6 regardless of the strain amplitude applied

(ii) an additional slip system was activated near the GB within the crystal G2[$\bar{1}25$] for all the RB bicrystals at strain amplitudes of 0·1% and 0·2%, and a GBAZ was formed. However, no secondary slip system was observed within the crystal G1[$\bar{4}79$], as shown in Fig. 3.

(iii) the width of the GBAZ containing secondary slip in the RB bicrystals, deformed at strain amplitudes of 0·1% and 0·2%, remained almost constant at 400 and 600 μm respectively, and was independent of the width of the bicrystals RB, as shown in Fig. 4*a* and *b*.

It is indicated that the plastic strain incompatibility near the GB is associated with the applied strain amplitudes

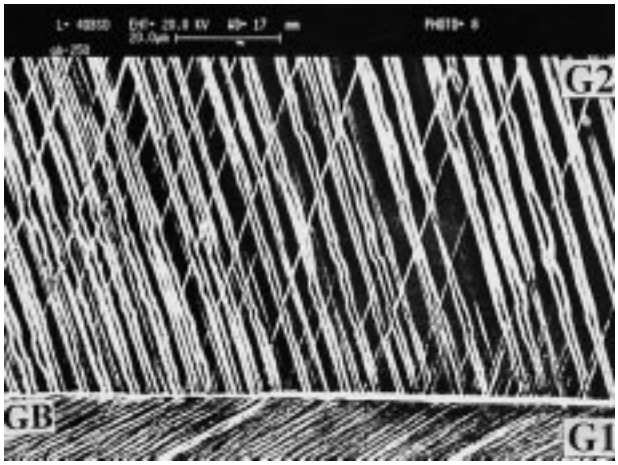

3 Slip morphology near grain boundary (GB) in RB bicrystal

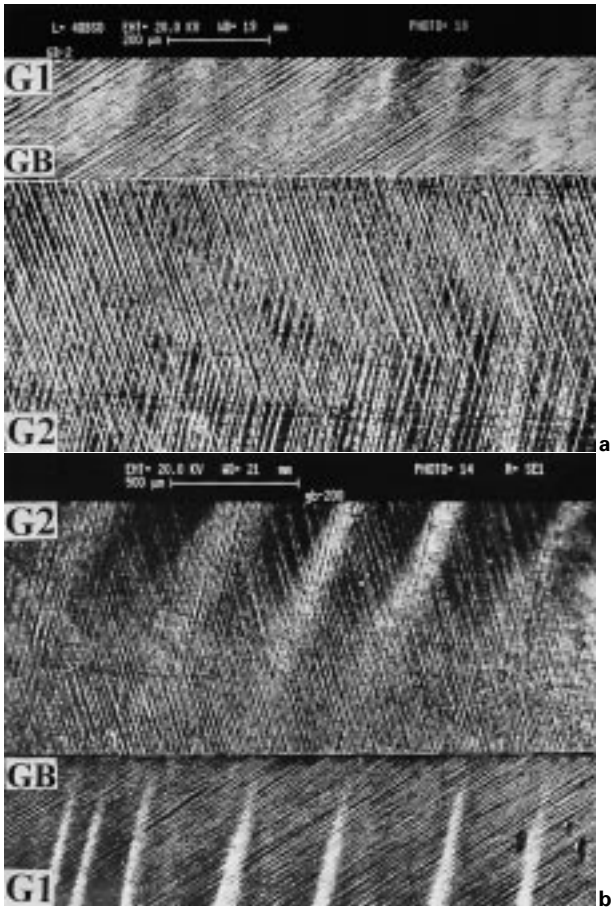

a $\varepsilon_{pl} = 0{\cdot}1\%$; *b* $\varepsilon_{pl} = 0{\cdot}2\%$

4 Grain boundary affected zone (GBAZ) in RB bicrystals at different strain amplitudes

under cyclic loading and is consistent with that in [$\bar{6}79$]‖[$\bar{1}45$] copper bicrystals.[22] In particular, the total number of the activated slip systems beside the GB was

Table 1 Axial saturation stress of combined (CB) and really grown (RB) copper bicrystals at given applied axial plastic strains ε_{pl}: $\Delta\sigma_{as} = \sigma_{as}^{RB} - \sigma_{as}^{CB}$

	σ_{as}, MPa		$\Delta\sigma_{as}$, MPa	
Specimen	$\varepsilon_{pl} = 1{\cdot}0 \times 10^{-3}$	$\varepsilon_{pl} = 2{\cdot}0 \times 10^{-3}$	$\varepsilon_{pl} = 1{\cdot}0 \times 10^{-3}$	$\varepsilon_{pl} = 2{\cdot}0 \times 10^{-3}$
CB-6	61·4	61·8	0	0
RB-8	64·5	65·4	3·1	3·6
RB-6	66·7	67·8	5·3	6·0
RB-4	69·4	70·9	8·0	9·1

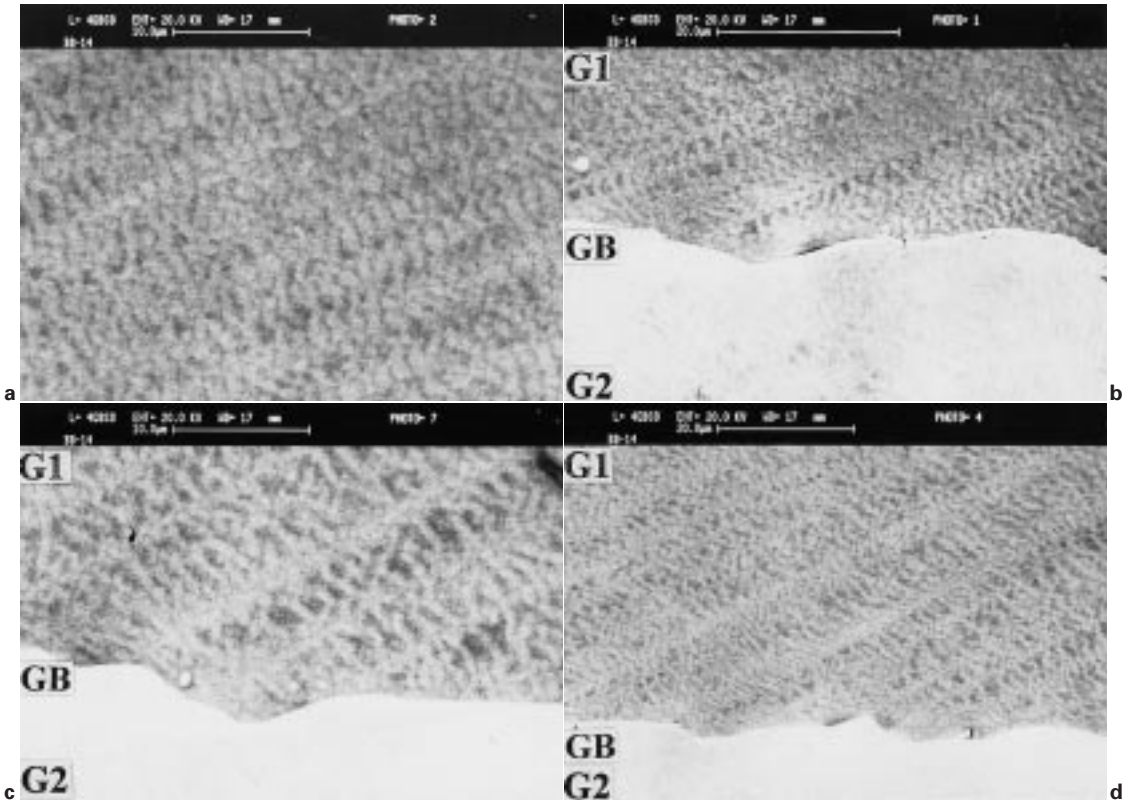

a in interior of crystal; *b–d* near grain boundary

5 Dislocation patterns observed by SEM-ECC technique in bicrystal RB-6: $\varepsilon_{pl} = 10^{-3}$

only equal to 3, not 4 as predicted by Kocks.[32] This might be because the orientations of the component crystals in the bicrystal are obviously different. The orientation of the crystal G2[$\bar{1}$25] is closer to the double slip, as shown in Fig. 1*c*, whereas, the G1[$\bar{4}$79] crystal is oriented for typical single slip so that the operation of secondary slip in it was more difficult than that of the crystal G2[$\bar{1}$25] after cyclic deformation. It is also confirmed that the operation of secondary slip near the GB produced by plastic strain incompatibility strongly depends on the crystal orientation.

DISLOCATION PATTERN OBSERVATION

To reveal the interaction of PSBs with the GB, the SEM-ECC technique was a direct and convenient method. The observations showed that the two phase structure of PSBs and matrix (or veins) can form in both the crystals G1 and G2 for all the CB and RB bicrystals deformed at strain amplitudes of 0·1% and 0·2%, as shown in Fig. 5*a*. In particular, these ladderlike PSBs within the crystal G1 can extend to the GB but cannot transfer through the GB, as shown in Fig. 5*b–d*, which is inconsistent with the surface slip morphology observations. However, the ladderlike PSBs within the crystal G2 cannot be observed in Fig. 5 owing to the difference in orientation and operation of secondary slip. In fact, the ladderlike PSB structure can only be observed on the lateral side within the crystal G2, but the interaction of PSBs with the GB within the crystal G2 cannot be revealed owing to the crystallographic relationships. These results further indicate that the SEM-ECC technique is an ideal method to investigate the fatigued dislocation patterns and two phase structure of PSBs and matrix that can form in these bicrystals during cyclic deformation. However, these are some shortcomings, such as in observing dislocation patterns near the GB by the SEM-ECC technique, the dislocation patterns beside a GB cannot be clearly observed simultaneously because of the misorientation of the adjacent grains, as shown in Fig. 5*b–d*.

Discussion

EFFECT OF GRAIN SIZE ON GB STRENGTHENING OF RB BICRYSTALS

The effect of GB on flow stress has been extensively discussed in bicrystals with the GB parallel to the stress axis.[13–20] Chuang and Margolin[18] have given the stress relation in isoaxial β brass bicrystals as

$$\sigma_T = \sigma_B + V_{GB}(\sigma_{GB} - \sigma_B) \quad . \quad . \quad . \quad . \quad . \quad . \quad . \quad . \quad . \quad . \quad (1)$$

where the average stress in GB deformation zone σ_{GB} can be determined from the measured value of applied stress σ_T, single crystal flow stress σ_B, and the volume fraction of GB deformation zone V_{GB}. The increased stress of the bicrystal is attributed to the high stress in the GB deformation zone. Similarly, Mirura and Saeki[16] and Mirura *et al.*[17] found that the flow stresses of bicrystals were also increased by the presence of $\Sigma 7$ and $\Sigma 21$ coincidence GBs. The stress, namely as GB strength, rapidly increased as a result of the interaction between primary slip and the additional slip in the vicinity of the GB.

One of the aims of the present work is to determine the grain size effect of GB strengthening on cyclic saturation stress in these RB bicrystals. Under cyclic loading, the GB will play a more striking role than under monotonic loading. By comparing the stress–strain responses of the bicrystals CB and RB, the strengthening effect of the GB is clearly shown in Fig. 2*a* and *b*. Surface observation also revealed a GBAZ with secondary slip in the RB bicrystals as shown in Figs. 3 and 4, which are similar to the observations by Rey and Zaoui.[14,15] However, there is no such GBAZ in the CB bicrystal. When taking the GBAZ into account, as shown in Fig. 6*a* and *b*, the saturation stresses in the bicrystals RB and CB can be expressed as

$$\sigma_{as}^{CB} = \sigma_{as}^{G1} V_{G1} + \sigma_{as}^{G2} V_{G2} \quad . \quad . \quad . \quad . \quad . \quad . \quad . \quad . \quad . \quad . \quad (2)$$

$$\sigma_{as}^{RB} = \sigma_{as}^{CB} + V_{GB}(\sigma_{as}^{GB} - \sigma_{as}^{CB}) \quad . \quad . \quad . \quad . \quad . \quad . \quad . \quad . \quad . \quad (3)$$

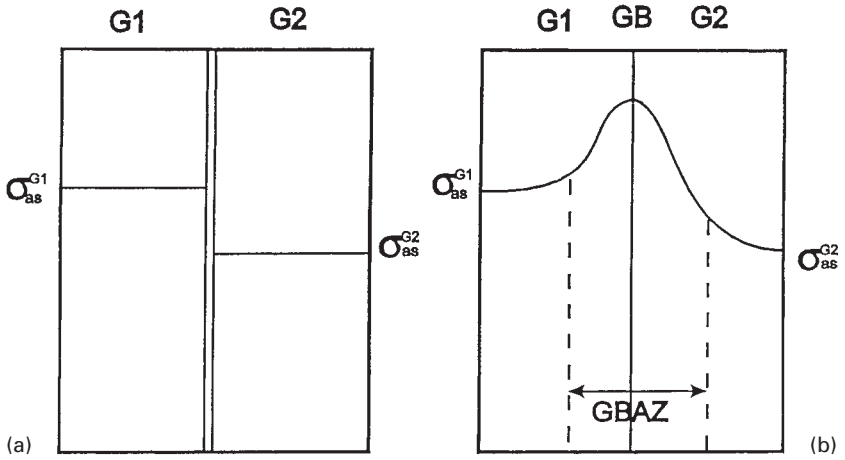

6 Schematic diagram of axial stress distribution in *a* CB and *b* RB bicrystals

where σ_{as}^{G1}, σ_{as}^{G2}, σ_{as}^{CB}, σ_{as}^{RB}, and σ_{as}^{GB} are the average axial saturation stresses in the component crystals (G1, G2), bicrystals (CB, RB), and the GBAZ, respectively; V_{G1}, V_{G2}, and V_{GB} are the volume fractions of component crystals (G1, G2), and the GBAZ. Here, V_{G1} and V_{G2} are equal to 0·5. By comparing the saturation stresses of the bicrystals CB and RB, as listed in Table 1, the difference in saturation stresses between the bicrystals CB and RB can be calculated using the relationship

$$\Delta\sigma_{as}^{B} = \sigma_{as}^{RB} - \sigma_{as}^{CB} \quad . . . . . (4)$$

where $\Delta\sigma_{as}^{B}$ is the average stress difference between the bicrystals CB and RB. The results are also listed in Table 1. Similar to the results by Chuang and Margolin,[18] the average stress difference $\Delta\sigma_B$ between the bicrystals RB and CB should be attributed to the high stress σ_{as}^{GB} in the GBAZ. Consequently, the saturation stresses of the bicrystals (RB-8, RB-6, and RB-4) are always higher than that of the bicrystal CB-6. From equation (3), the mean stress σ_{as}^{GB} in the GBAZ can be determined by the relationship

$$\sigma_{as}^{GB} = \frac{\sigma_{as}^{RB} - \sigma_{as}^{CB}}{V_{GB}} + \sigma_{as}^{CB} \quad . . . . . (5)$$

If W_B and W_{GB} are the widths of the specimen and the GBAZ in the RB bicrystals, respectively, the saturation stress of the bicrystals RB can be expressed as

$$\sigma_{as}^{RB} = \sigma_{as}^{CB} + (\sigma_{as}^{GB} - \sigma_{as}^{CB})(W_{GB}/W_B) \quad . . . . . (6)$$

Here, the width W_{GB} of the GBAZ in the bicrystals RB nearly maintained constant values of 400 and 600 μm, as shown in Fig. 4. However, the width W_B of the RB bicrystals are not constant and equal to 4, 6, and 8 mm. As a result, the saturation stress would be increased. This may be the reason why the saturation stress increased as the size of the bicrystals decreased (i.e. RB-8 < RB-6 < RB-4) at the same strain amplitude.

RESISTANCE OF GB ON PSBs

From the viewpoint of plastic deformation mechanism, the plastic strain in the component crystals and the bicrystals will be carried out by PSBs, as in copper single crystals.[1–3] Saturation dislocation observations confirmed that the PSBs can form in the bicrystals during cyclic deformation (Fig. 5). For the CB bicrystal, the saturation resolved shear stress on primary slip bands of the component crystals will be equal to that activating PSBs, as shown in Fig. 7*a*. However, the saturation resolved shear stress on the primary slip bands in the RB bicrystals may be different from that in the CB bicrystal owing to the GB strengthening effect. As shown in Fig. 7*b*, when the PSBs meet a GB, an additonal stress must be applied to the PSBs owing to the constraint of the GB. Therefore, it results in a higher saturation stress in the RB bicrystal than in the CB bicrystal. With increasing strain amplitude and reducing the width of the bicrystal RB, the difference in saturation stress between the bicrystals CB and RB will be increased. As reported previously,[22] by introducing an orientation factor Ω_B of the bicrystal

$$\Omega_B = \left(\frac{V_{G1}}{\Omega_{G1}} + \frac{V_{G2}}{\Omega_{G2}}\right)^{-1} \quad . . . . . (7)$$

where $\Omega_{G1} = 0{\cdot}436$ and $\Omega_{G2} = 0{\cdot}490$ are the Schmid factors of crystals G1 and G2, respectively. Thus, by using the data in Table 1, the saturation resolved shear stresses τ_{as}^{CB} and τ_{as}^{RB} of the bicrystals CB and RB can be calculated as

$$\left.\begin{aligned}\tau_{as}^{CB} &= \sigma_{as}^{CB}\Omega_B \\ \tau_{as}^{RB} &= \sigma_{as}^{RB}\Omega_B\end{aligned}\right\} \quad . . . . . (8)$$

The results are given in Table 2. It can be seen that the resolved shear stresses of the bicrystal CB-6 are equal to 28·3 and 28·5 MPa for the two applied strains, respectively, which are in good agreement with the stress activating PSBs in copper single crystals.[1–3] However, the resolved shear stresses of the RB bicrystals are obviously higher than 28–30 MPa. This implies that the increased resolved shear stresses must be attributed to the GB resistance to the PSBs in the RB bicrystals. By comparing saturation resolved shear stresses of the bicrystals CB and RB, as shown in Fig. 7, the GB resistance to the PSBs in the RB

Table 2 Resolved shear stress of combined (CB) and really grown (RB) copper bicrystals at given applied axial plastic strains ε_{pl}: $\Delta\tau_{as} = \tau_{as}^{RB} - \tau_{as}^{CB}$

	τ_{as}, MPa		$\Delta\tau_{as}$, MPa	
Specimen	$\varepsilon_{pl} = 1{\cdot}0 \times 10^{-3}$	$\varepsilon_{pl} = 2{\cdot}0 \times 10^{-3}$	$\varepsilon_{pl} = 1{\cdot}0 \times 10^{-3}$	$\varepsilon_{pl} = 2{\cdot}0 \times 10^{-3}$
CB-6	28·3	28·5	0	0
RB-8	29·7	30·1	1·4	1·6
RB-6	30·8	31·2	2·4	2·7
RB-4	32·0	32·7	3·7	4·2

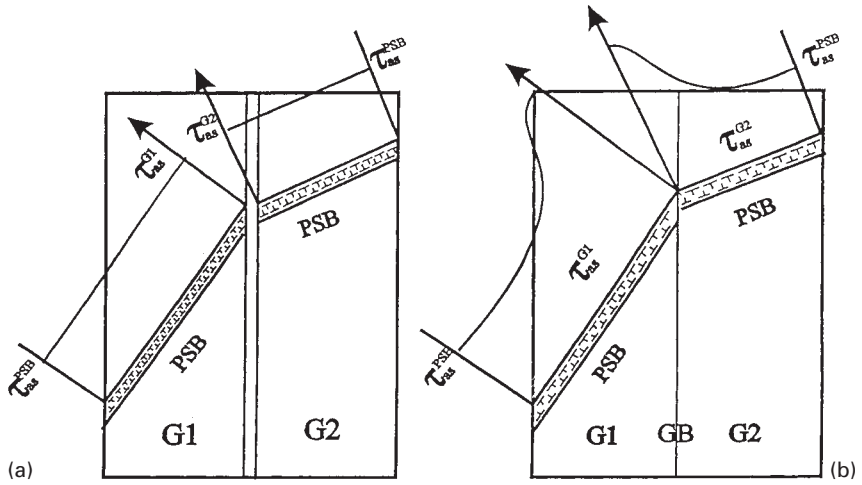

7 Schematic diagram of resolved shear stress distribution in *a* CB and *b* RB bicrystals

bicrystals can be introduced

$$\begin{aligned}\Delta\tau_{as}^{PSB} &= \tau_{as}^{RB} - \tau_{as}^{CB} \\ &= (\sigma_{as}^{RB} - \sigma_{as}^{CB})\Omega_B \\ &= \Delta\sigma_{as}^{B}\Omega_B \quad . \quad . \quad . \quad . \quad . \quad . \quad . \quad . \quad . \quad . \quad . \quad . \quad . \quad (9)\end{aligned}$$

As in Table 2, the mean GB resistance to the PSBs in the RB bicrystals also increased with decreasing the width of the RB bicrystals. Based on the results and discussion above, the GB strengthening effect on the RB bicrystals can be understood as follows. During cyclic deformation, the GB became a strong barrier to the slip bands, which cannot pass through the GB. Therefore, dislocation pile-up or plastic strain incompatibility will generate at the GB and result in stress concentration. With further cyclic deformation, secondary or multiple slip will operate near the GB, forming a GBAZ, as shown in Figs. 3 and 4. Consequently, the increase in saturation stress of the RB bicrystals should be associated with the GB resistance to the PSBs and the formation of the GBAZ with additional slip during cyclic deformation.

Conclusions

Based on the results above, the following conclusions can be drawn. Grain boundaries (GB) had strengthening effects on the really grown copper bicrystals (RB) with a parallel GB compared with the combined copper bicrystal (CB). The grain size effect of GB strengthening on RB bicrystals was discussed together with the GB affected zone (GBAZ) and the GB resistance to the persistent slip bands (PSBs). An additional slip system was activated near the GB within the crystal G2$[\bar{1}25]$ for all the RB bicrystals at strain amplitudes of 0·1% and 0·2%, which formed a GBAZ. However, no secondary slip system was observed within the crystal G1$[\bar{4}79]$. The SEM-ECC technique confirmed that the two phase structure of PSBs and matrix can form in these bicrystals during cyclic deformation, but these PSBs cannot transfer through the GB, which is inconsistent with the surface slip morphology observations.

Acknowledgement

The authors are grateful for the financial support of this work by the National Natural Science Foundation of China (NSFC) under Grant no. 5 19392300-4 and 59701006.

References

1. H. MUGHRABI: *Mater. Sci. Eng.*, 1978, **33**, 207–223.
2. Z. S. BASINSKI and S. J. BASINSKI: *Prog. Mater. Sci.*, 1992, **36**, 89–148.
3. A. S. CHENG and C. LAIRD: *Mater. Sci. Eng.*, 1981, **51**, 111–121.
4. S. P. BHAT and C. LAIRD: *Scr. Metall.*, 1978, **12**, 687–692.
5. K. V. RASMUSSEN and O. B. PEDERSEN: *Acta Metall.*, 1980, **28**, 1467–1478.
6. O. B. PEDERSEN and K. V. RASMUSSEN: *Acta Metall.*, 1982, **30**, 57–62.
7. V.-J. KUOKKALA, T. LEPISTO, and P. KETTUNEN: *Scr. Metall.*, 1982, **16**, 1149–1152.
8. H. MUGHRABI: *Scr. Metall.*, 1979, **13**, 479–484.
9. P. LUKAS and L. KUNZ: *Mater. Sci. Eng.*, 1985, **74**, L1–5.
10. A. T. WINTER: *Acta Metall.*, 1980, **28**, 963–964.
11. J. K. POHL, P. MAYR, and E. MACHERAUCH: *Scr. Metall.*, 1980, **14**, 1167–1169.
12. A. T. WINTER, O. B. PERDERSEN, and K. V. RASMUSSEN: *Acta Metall.*, 1981, **29**, 735–748.
13. P. LUKAS and L. KUNZ: *Mater. Sci. Eng. A*, 1994, **A189**, 1–7.
14. C. REY and A. ZAOUI: *Acta Metall.*, 1980, **28**, 687–697.
15. C. REY and A. ZAOUI: *Acta Metall.*, 1982, **30**, 523–535.
16. S. MIRURA and Y. SAEKI: *Acta Metall.*, 1978, **26**, 93–101.
17. S. MIRURA, K. HAMASHIMA, and K. T. AUST: *Acta Metall.*, 1980, **28**, 1591–1602.
18. Y.-D. CHUANG and H. MARGOLIN: *Metall. Trans. A*, 1973, **4A**, 1905–1917.
19. T.-D. LEE and H. MARGOLIN: *Metall. Trans A*, 1977, **8A**, 145–155.
20. T.-D. LEE and H. MARGOLIN: *Metall. Trans A*, 1977, **8A**, 157–167.
21. Y. M. HU, Z. G. WANG, and G. Y. LI: *Mater. Sci. Eng. A*, 1996, **A208**, 260–269.
22. Z. F. ZHANG and Z. G. WANG: *Acta Mater.*, 1998, **46**, 5063–5072.
23. D. MELISOVA, B. WEISS, and R. STICKLER: *Scr. Mater.*, 1997, **36**, 1061–1066.
24. D. R. G. MITCHELL and R. A. DAY: *Scr. Mater.*, 1998, **39**, 923–930.
25. A. SCHWAB, J. BRETSCHNEIDER, C. BUQUE, C. BLOCHWITZ, and C. HOLSTE: *Philos. Mag. Lett.*, 1996, **74**, 449–454.
26. A. SCHWAB, O. MEIßNER, and C. HOLSTE: *Philos. Mag. Lett.*, 1998, **77**, 23–31.
27. A. J. WILKINSON, M. B. HENDERSON, and J. W. MARTIN: *Philos. Mag. Lett.*, 1996, **74**, 145–151.
28. A. J. WILKINSON and P. B. HIRSCH: *Philos. Mag. A*, 1995, **74A**, 81–103.
29. R. ZAUTER, F. PETRY, M. BAYERLEIN, C. SOMMER, H.-J. CHRIST, and H. MUGHRABI: *Philos. Mag. A*, 1992, **66A**, 425–436.
30. Z. F. ZHANG and Z. G. WANG: *Philos. Mag. Lett.*, 1998, **78**, 105–113.
31. Z. F. ZHANG and Z. G. WANG: *Philos. Mag. A*, 1999, **79**, 741–752.
32. U. F. KOCKS: *Philos. Mag. A*, 1964, **9A**, 187–193.